28. Stoffers, P., Glasby, G. P. and Frenzel, G., Comparison of the characteristics of manganese micronodules from the equatorial and southwest Pacific. *Tscher. Miner. Petrog.*, 1984, **33**, 1–23.
29. Froelich, P. N. *et al.*, Early oxidation of organic matter in pelagic sediments of the eastern and equatorial Atlantic: sub-oxic diagenesis. *Geochim. Cosmochim. Acta*, 1979, **43**, 1075–1090.
30. Postma, D. and Jakobsen, R., Redox zonation: equilibrium constrains on the Fe(III)/SO_4-reduction interface. *Geochim. Cosmochim. Acta*, 1996, **60**, 3169–3175.
31. Lynn, D. C. and Bonatti, E., Mobility of manganese in diagenesis of deep sea sediments. *Mar. Geol.*, 1965, **3**, 457–474.
32. Chakraborty, P., Chakraborty, S., Jayachandran, S., Madan, R., Sarkar, A., Linsy, P. and Nagender Nath, B., Effects of bottom water dissolved oxygen variability on copper and lead fractionation in the sediments across the oxygen minimum zone, western continental margin of India. *Sci. Total Environ.*, 2016, **556**, 1052–1061.
33. Pattan, J. N., Parthiban, G., Prakash Babu, C., Khadge, N. H., Paropkari, A. L. and Kodagali, V. N., A note on geochemistry of surface sediments from Krishna–Godavari basin, east coast of India. *J. Geol. Soc. India*, 2008, **71**, 107–114.
34. Prakash Babu, C. and Ramaswamy, V., Phosphorus accumulation associated with intense diagenetic metal-oxide cycling in sediments along the eastern continental margin of India. *Curr. Sci.*, 2017, **113**(3), 473–478.
35. Burns, R. G. and Burns, V. M., Authigenic oxides. In *The Sea, Volume 7, The Oceanic Lithosphere* (ed. Emiliani, C.), Wiley-Interscience, New York, USA, 1981, pp. 875–914.
36. Balistrieri, L. S. and Murray, J. W., The surface chemistry of sediments from the Panama Basin: the influence of Mn oxides on metal adsorption. *Geochim. Cosmochim. Acta*, 1986, **50**, 2235–2243.
37. Subramanian, V., 'T Dack, L. V. and Grieken, R. V., Chemical composition of river sediments from the Indian sub-continent. *Chem. Geol.*, 1985, **48**, 271–279.

ACKNOWLEDGEMENTS. We thank the Director, NIO, Goa for permission to publish this paper. We also thank the anonymous reviewers for constructive comments that helped improve the manuscript. Discussions with J. N. Pattan, NIO, Goa helped us understand manganese micronodules formation. We thank G. Parthiban, NIO, Goa for help during ICP-OES analysis and V. D. Khedekar and Areef Sardar, NIO, Goa for assistance during SEM and EPMA. This work is a part of NIO's 12th Five-Year Plan approved project 'Geosinks'. This is NIO's contribution No. 6151.

Received 27 February 2017; revised accepted 5 January 2018

doi: 10.18520/cs/v114/i10/2161-2167

Estimation of rock load in development workings of underground coal mines – a modified RMR approach

Avinash Paul[1,*], Vemavarapu Mallika Sita Ramachandra Murthy[2], Amar Prakash[1] and Ajoy Kumar Singh[1]

[1]Central Institute of Mining and Fuel Research, Dhanbad 826 015, India
[2]Department of Mining Engineering, Indian Institute of Technology (Indian School of Mines), Dhanbad 826 004, India

Underground coal mining in India contributes to a share of 55 Mt production with more than 500 mines in operation. In spite of using the well-established CMRI-ISM Rock Mass Rating (RMR_{dyn}) classification system for roof support design successfully in Indian geo-mining conditions, accidents due to roof fall constitute the major challenge. These failures are generally due to the presence of weak beddings and laminations. Seismic refraction technique (for shallow depth) can be useful in detecting the rock mass conditions. Based on the study a modified rock mass classification system (RMR_{dyn}) was setup by incorporating field *P*-wave velocity with a view to arrive at a real ground condition of the *in situ* rock. Rock loads were also determined in the field to develop a relation with RMR_{dyn}. A comparison of rock load estimation by CMRI-ISM RMR, numerical simulation and RMR_{dyn} clearly depicts that the latter approach is more reliable as the results are close to the actual scenario.

Keywords: CMRI-ISM RMR, RMR_{dyn}, *P*-wave velocity, rock load, support design.

ROCK mass classification systems have constituted an integral part of empirical mine design for over 100 years[1]. An important contribution of the rock mass rating (RMR) is that the system has stimulated the development of a plethora of more specialized systems of ground evaluation, particularly in mining application[2]. It provides guidelines for stability assessment and also to select the appropriate support system[3].

Ground movement is a serious concern in underground coal mines[4]. Roof fall generally takes place due to detachment of lower strata since the redistribution of stresses takes place around the excavation made[5]. Blasting in the development faces is also one of the major causes of roof damage due to lack of free face and consequent higher order ground vibrations[6]. The strength of roof rock can be improved by installing timely supports with adequate capacity[7,8]. Thus, proper rock load assessment and support design for mine openings are considered as major factors in the stability of the roof strata[9,10].

*For correspondence. (e-mail: avinashpaul02@yahoo.co.in)

In situ seismic refraction is a technique used in the coal mine roof to determine the seismic wave velocity and the extent of weak zones in the surrounding rock[11]. In seismic characterization, the basic procedure is to generate seismic waves by a near-surface hammering, and record through geophones the resulting waves which reach the surface of the roof at different places after travelling through different paths. The positions of reflecting and refracting interfaces are deduced by analysis of the travel times of identifiable wave groups[12].

As *in situ* rock exhibits DIANE behaviour (discontinuous, inhomogeneous, anisotropic and non-linearly elastic) and by using the laboratory resulted factors like uniaxial compressive strength, knowledge about the occurrence and strength of the rock fracture gets delineated[13–15]. *In situ P*-wave velocity has been proved as a better option than compressive strength factor owing to two major grounds. First, it is calculated in field and thus takes into account *in situ* conditions (including the true conditions such as structure, stress and strength). Measurement of *in situ P*-wave velocity is a significant way to determine mechanical parameters of rock mass[16,17]. It is useful for the purpose of rock mass characterization, including the influence of virgin and induced stresses in their entirety. Secondly, it envelops an area larger than the preceding one, thus being more representative. The eminent use of this technique is in the selection of the required support system. Counting on a formulation that contains majority of field-estimated factors, rock mass rating (RMR_{dyn}) will help in classifying the rocks more precisely and aid in selecting the suitable support system required, thus making it more viable from economics viewpoint also. The present study suggests a new system of rating applying seismic imaging technique by replacing the compressive strength factor in Central Mining Research Institute–Indian School of Mines Rock Mass Rating (CMRI-ISM RMR).

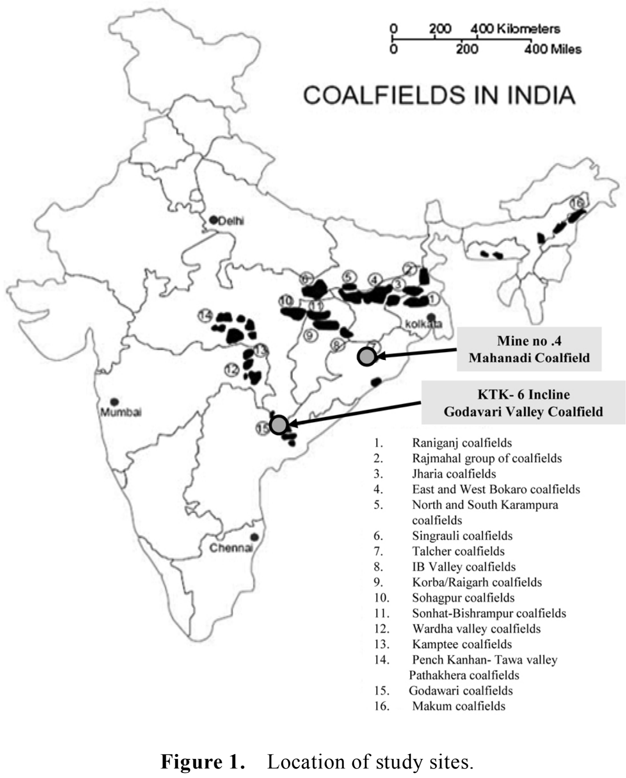

Figure 1. Location of study sites.

The study was conducted at sites 24L/15DJ and 38L/15DJ of mine no. 4 of Mahanadi Coalfield and at site 13LN/B of KTK–6 Incline mine of Godavari Valley Coalfield (Figure 1).

These sites were selected emphasizing the area subjected to bad and friable roof conditions in benefit of mine management for proper support design for safe workings. At 24L/15DJ of mine no. 4, the immediate roof was composed of coal and overlain by shale and sandstone, whereas at 38L/15DJ the roof was composed of sandstone. At places, slips and random joints were also observed in the sandstone layer. Mine roof was dry. At 13LN/B of KTK-6 Incline mine, the roof was composed of medium-grained sandstone. Random joints with occasional slips were observed in the sandstone. Heavy seepage of water was also observed.

Seismic imaging was done using Handy Viewer McSEIS-3 (MODEL-1817). In Figure 2, Z_0, Z_1 and Z_2 represent different layers in the roof, and V_0, V_1 and V_2 are the corresponding seismic velocities. Seismic waves generated at point *S* travel in hemispherical form and are received by three geophones installed in the roof at predetermined distances. The rating of field *P*-wave velocity (c_{pi}), obtained by trial and error method was used to determine RMR_{dyn} (Table 1).

Time to distance curves were plotted for the three study sites to determine *P*-wave velocity of different strata (Figures 3–5). The *P*-wave velocity at all the sites showed an increasing trend towards the inner part of the roof, which clearly depicted that the immediate roof was weak in comparison to the inner strata (Table 2).

RMR of roof rocks using CMRI-ISM geomechanical classification system[18] was determined by measuring five parameters, i.e. layer thickness, structural features, slake durability, uniaxial compressive strength and groundwater condition at all the three sites (Tables 3–5). Combined RMR was computed using the following formula

$$\text{Combined RMR} = [(A \times X) + (B \times Y) + (C \times Z)]/ A + B + C),$$

where *X*, *Y* and *Z* are RMRs of rock mass, and *A*, *B* and *C* are their respective values of thickness (m).

Adjusted RMR was computed considering 10% reduction for blasting-off-solid and accordingly, status of roof condition was assessed (Table 6). Utilizing the key parameters of CMRI-ISM geomechanical classification system and using *in situ P*-wave velocity in place of

Table 1. Rating used for *P*-wave velocity[6]

P-wave velocity (m/s)	<1000	1000–2000	2000–3000	3000–3500	>3500
Rating	0–5	6–10	11–14	15–17	18–20

Table 2. Determination of *P*-wave velocity at different sites

Parameters	24L/15DJ			38L/15DJ		13LN/B		
Geophone number	G1	G2	G3	G1	G2	G1	G2	G3
Distance from source (m)	1.66	3.68	5.72	3.56	5.48	1.35	2.95	4.72
First arrival time (ms)	1.47	2.91	3.80	2.82	3.80	1.20	2.50	3.60
P-wave velocity (m/s)	$V_0 = 1129$	$V_1 = 1407$	$V_2 = 1959$	$V_0 = 1265$	$V_1 = 1872$	$V_0 = 1125$	$V_1 = 1333$	$V_2 = 2082$

V_0 = 1/Slope of first line; V_1 = 1/Slope of second line; V_3 = 1/Slope of third line.

Table 3. Calculation of CMRI-ISM RMR for 24L/15DJ site

	Coal		Shale		Sandstone	
Parameter	Value	Rating	Value	Rating	Value	Rating
Layer thickness (cm)	5.2	10	4.85	9	10.6	16
Structural features (cleats/slips)	10	12	9	13	11	10
Weatherability (%)	93.85	12	93.93	12	89.26	10
Compressive strength (kg/cm^2)	148.7	03	174.7	4	54.4	01
Groundwater (ml/min)	Dry	10	Dry	10	Dry	10
RMR	47		49		47	

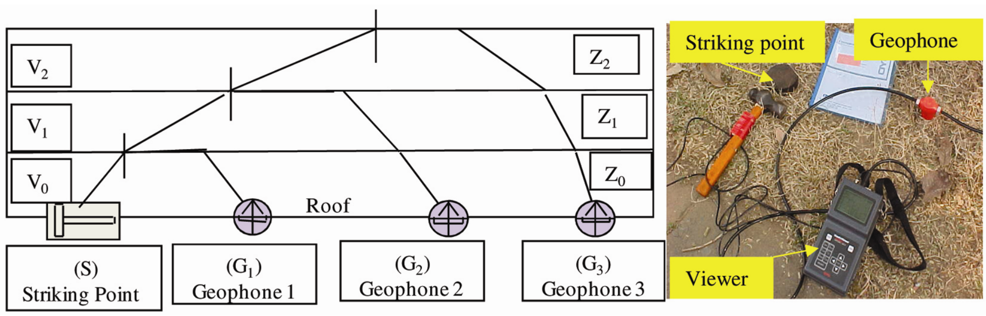

Figure 2. Seismic imaging measurement technique.

uniaxial compressive strength the new RMR_{dyn} was computed for the three study areas (Tables 7–9) with the same geo-mining conditions (Table 6). As the *in situ* *P*-wave velocity represents the actual rock mass condition, RMR_{dyn} was not adjusted. *P*-wave velocity in all the beds was greater than 1000 m/s, and hence, the fourth bed is more competent based on the principle that higher the *P*-wave velocity, more competent is the rock mass. Thus, weak roof was considered up to third layer only. Status of roof conditions is based on RMR_{dyn} (Table 10). RMR_{dyn} values were observed to be on a higher side in relation to CMRI-ISM RMR for all the three sites, especially for the fair-to-poor roof conditions.

The rock load height can be calculated in three ways: (a) by measuring the length of exposed bolt; (b) by determining the height of weak horizon in roof rock between the roof and the weak layer, i.e. lithological section, and (c) by measuring the length of extent of roof fall. Rock load height in development galleries was determined based on the lithological section (extent of weak layers) of the immediate mine roof (Figure 6). Rock load was determined as a product of rock load height and density of rock (Table 11).

With the CMRI-ISM RMR system, rock load for development galleries was calculated using the following relation

$$\text{Rock load in gallery (t/m}^2\text{)} = B.\gamma*[1.7 - 0.037*\text{RMR} + 0.0002*\text{RMR}^2], \quad (1)$$

where B is the roadway width (m) and γ is the dry density (t/m^3).

Table 12 gives the values of rock load at different locations. Rock load for development galleries was calculated by RMR_{dyn} system using the following relation

Rock load in gallery (t/m²)

$$= B.\gamma*[1.456 - 0.017*\mathrm{RMR}_{\mathrm{dyn}}], \quad (2)$$

where B and γ are the same as in eq. (1).

The rock load equation developed by correlating $\mathrm{RMR}_{\mathrm{dyn}}$ with the actual rock load values obtained in field (Table 11). Table 13 gives the values of rock load at different locations.

Numerical modelling was done using 3D finite difference software, FLAC^{3D}. The geometry and geo-mining data (Young's modulus, Poisson's ratio, density of rock and intact compressive strength) were chosen based on prevailing geo-mining conditions (Tables 14 and 15). The relations used for determining the horizontal *in situ* stresses and vertical stresses are

$$S_h = 2.0 + 0.01H \text{ (in situ horizontal stresses)}, \quad (3)$$

$$S_v = 0.025H \text{ (vertical stresses)}. \quad (4)$$

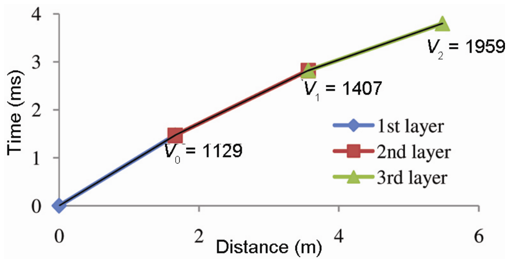

Figure 3. Time versus distance curve at 24L/15DJ.

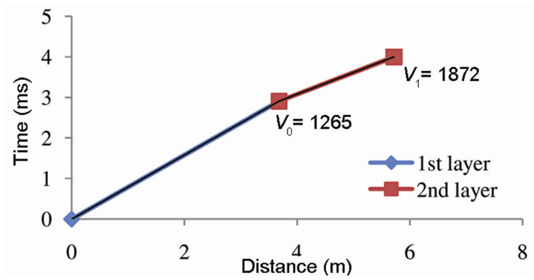

Figure 4. Time versus distance curve at 38L/15DJ.

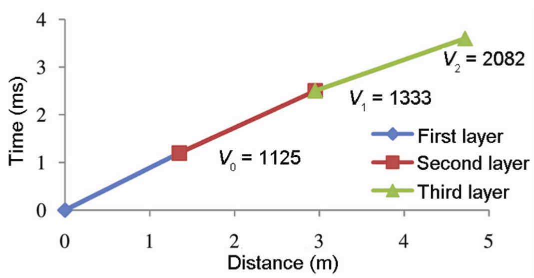

Figure 5. Time versus distance curve at 13LN/BD.

Table 4. Calculation of CMRI-ISM RMR for 38L/15DJ site

	Sandstone	
Parameter	Value	Rating
Layer thickness (cm)	10.6	16
Structural features (cleats/slips)	10	09
Weatherability (%)	89.26	10
Compressive strength (kg/cm²)	50.8	01
Groundwater (ml/min)	Dry	10
RMR	46	

Drivages of 4.2 m × 2.7 m, 3.6 m × 2.8 m and 4.2 m × 2.7 m were driven for the respective locations of 24L/15DJ, 13LN/B and 38L/15DJ for the formation of pillars in coal and drift in stone. Stability of the immediate roof was assessed by safety factors represented by different colour contours at different heights (Figure 7). The blue colour contour from 0.5 to 1 in Figure 7 shows unstable zone height.

The safety factor contours obtained in the location 24L/15DJ, HR top seam for galleries were less than 1.0 and extended up to the height of 1.5 m. Thus, the rock load is expected to get mobilized up to a height of 1.5 m in the immediate roof and thus needs to be supported. Rock load obtained from modelling was 2.46 t/m² after multiplying rock load height with density for RMR 47.25. Similarly, rock load height obtained by simulation at 38L/15DJ and 13LN/B was 1.0 m and 2.0 m respectively, and the corresponding rock load and RMR values obtained were 2.15, 46 and 4.16 and 36.7 t/m², respectively.

The values of rock load obtained by different estimation methods vary from actual field observations (Tables 7–11). Rock load was compared by RMR estimated using different techniques (Table 16 and Figure 8).

Rock load curve for $\mathrm{RMR}_{\mathrm{dyn}}$ was found to be on upper side, i.e. rock load is highest for $\mathrm{RMR}_{\mathrm{dyn}}$. For instance, at RMR value of 40 the rock loads are around 6.9, 4.8 and 2.9 t/m² by $\mathrm{RMR}_{\mathrm{dyn}}$, CMRI-ISM RMR and numerical modelling respectively. Rock load value was found to reduce significantly after RMR value of 42. The rock load values determined by $\mathrm{RMR}_{\mathrm{dyn}}$ were found to be in close approximation with the actual values (Figure 9). Significant deviation was observed by numerical modelling owing to the fact that theoretical horizontal stresses were arrived based on established empirical relation between horizontal *in situ* stress and depth of cover for coal measures[19] due to absence of actual measurements of *in situ* stresses.

RMR determination by replacing compressive strength of rock with *P*-wave velocity incorporates the *in situ* condition of the rock for evaluating precise rock load. The value of rock load obtained from CMRI-ISM RMR was less for low RMR values (Figure 8), compared to the rock load obtained by $\mathrm{RMR}_{\mathrm{dyn}}$ leading to underestimation of rock load. This may be attributed to the difference in the method of assessing rock strength, adjustments

Table 5. Calculation of CMRI-ISM RMR for 13LN/B site

	Coarse-grained sandstone		Coarse-grained sandstone		Medium- to coarse-grained sandstone		Medium- to coarse-grained sandstone	
Parameter	Value	Rating	Value	Rating	Value	Rating	Value	Rating
Layer thickness (cm)	12	15	20	20	15	17	20	20
Structural features (cleats/slips)	12	6	12	6	12	6	12	6
Slake durability index (%)	97	14	75	6	56	3	55	3
Compressive strength (kg/cm^2)	849	12	151	4	83	2	131	3
Groundwater seepage rate (ml/min)	500–6000	0	500–6000	0	500–6000	0	500–6000	0
RMR	47		36		28		32	

Table 6. Roof condition based on CMRI-ISM RMR

Site	Geo-mining condition	Rock type	RMR	Combined RMR	Adjusted RMR	Roof condition
24L/15DJ	Immediate roof was coal and overlain by shale and sandstone.	Coal	47	47.25	42.75	Fair
	Presence of joints/cleats and occasional slips.	Shale	49			
	Two sets of cleat (N75° and N165°) were prominent in coal.	Sandstone	47			
	Cleat spacing was 10-30 cm.					
	Dry roof condition.					
38L/15DJ	Immediate roof was sandstone with existence of joints.	Sandstone	46	46	41.4	Fair
	Presence of occasional slips.					
	Dry roof condition.					
13LN/B	Immediate roof was sandstone with existence of joints.	Coarse-grained sandstone	47	36.7	33	Poor
		Coarse-grained sandstone	36			
	Presence of occasional slips.	Medium- to coarse-grained sandstone	28			
	Dry roof condition.	Medium- to coarse-grained sandstone	32			

Table 7. Calculation of RMR_{dyn} for 24L/15DJ site

	Coal		Shale		Sandstone	
Parameter	Value	Rating	Value	Rating	Value	Rating
Layer thickness (cm)	5.2	10	4.85	09	10.6	16
Structural features (cleats/slips)	10	12	9	13	11	10
Weatherability (%)	93.85	12	93.93	12	89.26	10
P-wave velocity (m/s)	1129	06	1404	07	1959	11
Groundwater	Dry	10	Dry	10	Dry	10
RMR	50		51		57	

Table 8. Calculation of RMR_{dyn} for 38L/15DJ site

	Sandstone	
Parameter	Value	Rating
Layer thickness (cm)	10.6	16
Structural features (cleats/slips)	10	09
Weatherability (%)	89.26	10
P-wave velocity (m/s)	1265	07
Groundwater	Dry	10
RMR	52	

suggested to account for blast damage, depth, width of gallery, etc. Thus, rock load determination by RMR_{dyn} was found to be more reliable among all the methods.

RMR_{dyn} avoids repeated adjustments by adopting a quantitative approach for rock mass characterization. For lower RMR values, the rock loads could be higher whereas for higher RMR values the rock loads could be lower (Figure 8) due to difference in the degree of damage inflicted by blasting-off-solid. This leads to unsafe support design to over-safe designs, which can be rationalized using RMR_{dyn} approach.

It has been observed in practice that for RMR values less than 40, roof stability problems occur while designing support system using CMRI-ISM rock mass classification system. The main cause for this may be due to the lower rock loads predicted, thus providing lower support density. Considering this limitation, RMR_{dyn}-based rock loads were used to design supports in the mines of

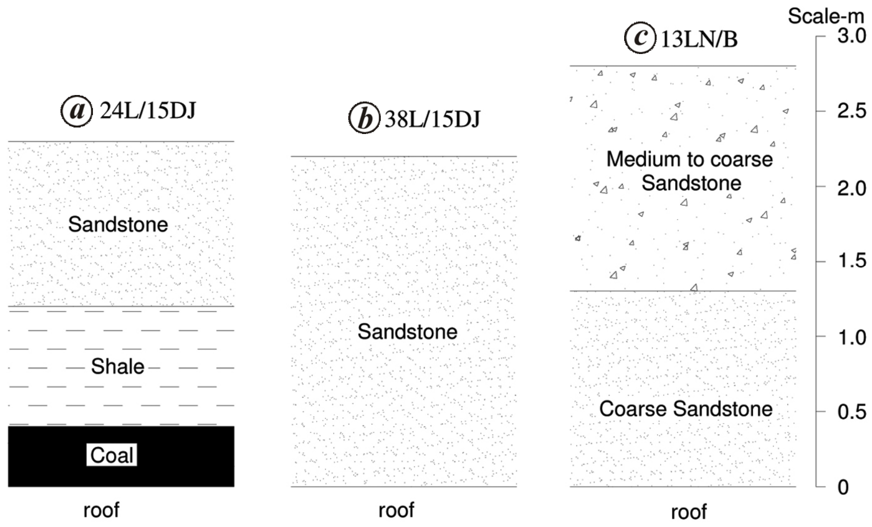

Figure 6. Lithological section above the roof showing extent of weak layers.

Table 9. Calculation of RMR_{dyn} for 13LN/B site

	Coarse-grained sandstone		Coarse-grained sandstone		Medium- to coarse-grained sandstone		Medium- to coarse-grained sandstone	
Parameter	Value	Rating	Value	Rating	Value	Rating	Value	Rating
Layer thickness (cm)	12	15	20	20	15	17	20	20
Structural features (cleats/slips)	12	6	12	6	12	6	12	6
Slake durability index (%)	97	14	75	6	56	3	55	3
P-wave velocity (m/s)	1125	6	1333	7	2082	11	2082	8
Ground water seepage rate (ml/min)	500–6000	0	500–6000	0	500–6000	0	500–6000	0
RMR	41		39		37		40	

Table 10. Roof condition based on RMR_{dyn}

Site	Rock-type	RMR_{dyn}	Combined RMR_{dyn}	Roof condition
24L/15DJ	Coal	50	54.1	Fair
	Shale	51		
	Sandstone	57		
38L/15DJ	Sandstone	52	52	Fair
13LN/B	Coarse-grained sandstone	41	39.5	Poor
	Coarse-grained sandstone	39		
	Medium- to coarse-grained sandstone	37		
	Medium- to coarse-grained sandstone	40		

Table 11. Rock load based on roof lithology

Location	Rock load height (m)	Density (t/m^3)	Rock load (t/m^2)
24L/15DJ	2.30	1.64	3.77
38L/15DJ	2.20	2.15	4.73
13LN/B	2.80	2.08	5.82

Godavari Valley Coalfield and Mahanadi Coalfield with better stability. The CMRI-ISM rock mass classification system postulates an overall RMR reduction of 10% due to blasting-off-solid, which is eliminated by the newly suggested system as it takes into account the actual rock mass condition existing *in situ*.

This study presents a new approach for estimation of rock load in development galleries of coal mines based on seismic imaging of roof. Field *P*-wave velocity has been found to characterize the rock mass in a better way for assessing its competency. For a given rock load, the conventional CMRI-ISM RMR values were found to be on lower side in comparison to RMR_{dyn} values at lower range of rock mass rating, which signifies that rock load

Table 12. Determination of rock load by CMRI-ISM RMR

Location	RMR	Gallery width (m)	Density (t/m^3)	Rock load height (m)	Rock load (t/m^2)
24L/15DJ	42.75	4.2	1.64	2.03	3.33
38L/15DJ	41.4	4.2	2.15	2.15	4.61
13LN/B	33	3.6	2.08	2.51	5.22

Table 13. Determination of rock load by RMR_{dyn}

Location	RMR_{dyn}	Gallery width (m)	Density (t/m^3)	Rock load height (m)	Rock load (t/m^2)
24L/15DJ	54.1	4.2	1.64	2.25	3.69
38L/15DJ	52.0	4.2	2.15	2.40	5.16
13LN/B	39.5	3.6	2.08	2.82	5.87

Table 14. Geometry given for numerical models

Sites	Seam thickness (m)	Extraction height (m)	Pillar size (m^2)	Depth (m)	Gallery width (m)
24L/15DJ	3.4	2.7	22 m × 22 m	70	4.2
13LN/B	2.8	2.8	20 m × 20 m	82	3.6
38L/15DJ	3.4	2.7	22 m × 22 m	122	4.2

Table 15. Input parameters used for numerical modelling

Site	Rocks (immediate roof of 2m)	Modulus of elasticity (GPa)	Poisson's ratio	Rock density (kg/m^3)	Intact compressive strength (MPa)	*b*	RMR
24L/15DJ	Sandstone	Sandstone(5.0)	Shale (0.25)	Coal (1.24)	Coal (37.4)	0.5	47.25
	Shale	Shale (2.0)	Coal (0.25)	Shale (1.35)	Shale (22.7)		
	Coal	Coal (2.0)	Sandstone (0.30)	Sandstone (1.94)	Sandstone (23.3)		
13LN/B	Sandstone	Sandstone (5.0)	Sandstone(0.25)	Sandstone (2.15)	Sandstone (25.2)	0.5	37
	Coal	Coal (2.0)	Coal (0.25)	Coal (1.4)	Coal (30.3)		
38L/15DJ	Sandstone	Sandstone (5.0)	Sandstone (0.30)	Sandstone (2.0)	Sandstone (33)	0.5	46

Table 16. Rock load and RMR value of the three sites

	CMRI-ISM RMR		Numerical model		RMR_{dyn}	
Location	RMR	Rock load (t/m^2)	RMR	Rock load (t/m^2)	RMR	Rock load (t/m^2) (from eq (5))
24L/15DJ, mine no. 4 MCL	42.7	3.33	47.25	2.46	54.1	3.69
KTK-6 incline	33	5.22	36.7	4.16	40	5.87
38L, mine no. 4 MCL	41.4	4.61	46	2.15	52	5.16

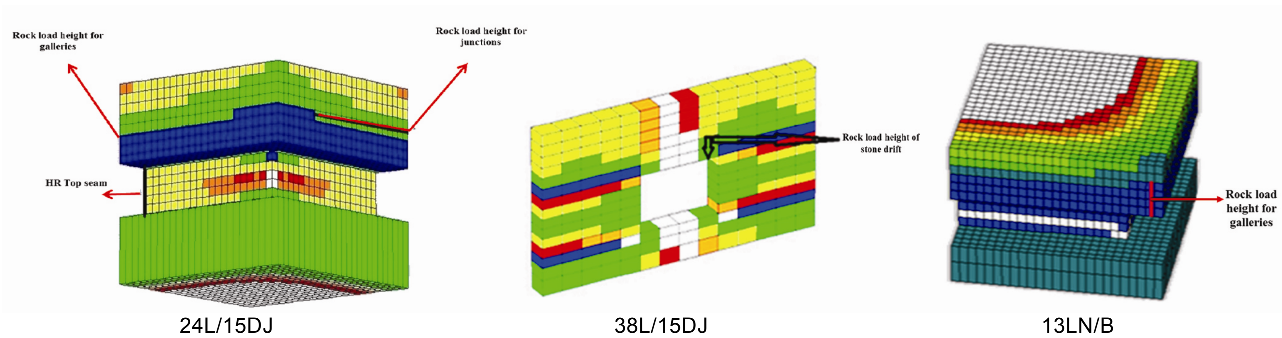

Figure 7. Numerical model showing rock load height.

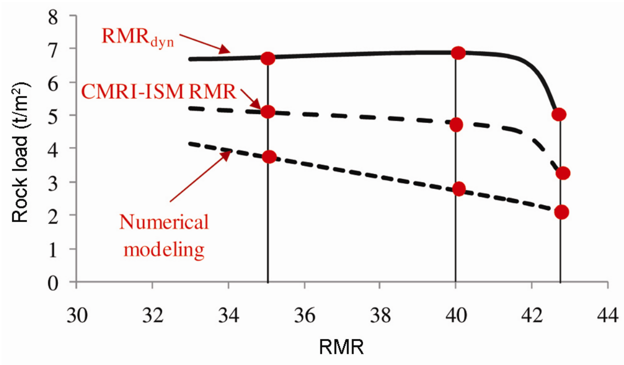

Figure 8. Rock load under various estimated RMRs.

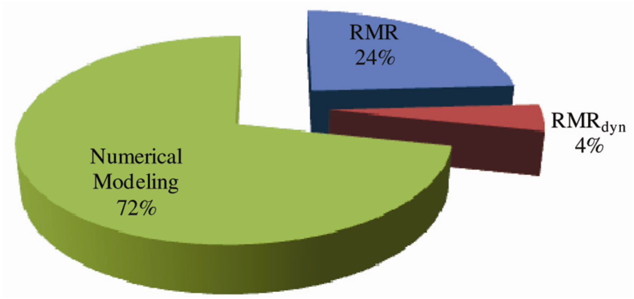

Figure 9. Percentage deviation of rock load estimated by different methods.

values are underestimated by CMRI-ISM RMR and numerical modelling approaches. The rock loads estimated using the three approaches find reasonable correlation, with RMR_{dyn} predicting higher values in comparison to the other approaches. The suggested RMR_{dyn} classification system considers the key rock mass features and estimates rock loads which can lead to more effective and economic designs. This approach has been applied to limited cases and therefore requires extensive studies for further validation.

1. Ritter, W., *Die Static der Tunnelgewolbe*, Springer, Berlin, 1879.
2. Cummings, R. A., Kendorski, F. S. and Bieniawski, Z. T., Caving rock mass classification and support estimates. USBM Contract Report I0100103, Engineers International Inc, Chicago, USA, 1982.
3. Bieniawski, Z. T., Engineering classification of jointed rock mass. *Trans. South Afr. Civ. Eng.*, 1973, **15**, 335–344.
4. Ghosh, C. N. and Ghose, A. K., Estimation of critical convergence and rock load in coal mine roadways – an approach based on rock mass rating. *Geotech. Geol. Eng.*, 1992, **10**, 185–202.
5. Paul, A., Singh, A. P., John, L. P., Singh, A. K. and Khandelwal, M., Validation of RMR-based support design using roof bolts by numerical modeling for underground coal mine of Monnet Ispat, Raigarh, India – a case study. *Arab. J. Geosci.*, 2011; doi:10.1007/s12517-011-0313-8.
6. Suresh, R. and Murthy, V. M. S. R., Seismic characterization of coal mine roof for rock load assessment. In First Indian Mineral Congress, Dhanbad, 2005, pp. 31–46.
7. Laubscher, D. H., Planning mass mining operations. In *Comprehensive Rock Engineering* (ed. Hudson, J. A.), Pergamon Press, Oxford, UK, 1993, vol. 2, pp. 547–583.
8. Hudson, J. A. and Harrison, J. P., *Engineering Rock Mechanics – An Introduction to Principles*, Pergamon, An imprint of Elsevier Science, Amsterdam, The Netherlands, 1997, pp. 314–315.
9. Paul, A., Singh. A. K., Sinha, A. and Saikia, K., Geotechnical investigation for support design in Depillaring panels in Indian coal mines. *J. Sci. Ind. Res.*, 2005, **64**, 358–363.
10. Paul, A., Singh, A. K., Rao, D. G. and Kumar, N., Empirical approach for estimation of rock load in development workings of room and pillar mining. *J. Sci. Ind. Res*., 2009, **68**, 214–216.
11. Scott, D. F., Williams, T. J., Denton, D. K. and Friedel, M. J., Seismic tomography as a tool for measuring stress in mines. *Min. Eng*., 1990, **51**(1), 77–80.
12. Singh, K. K. K., In-seam seismic application for detecting inhomogeneities in coal seams – a review. *J. Min. Met. Fuel*, 1994, 49–54.
13. Barton, N. R., Lien, R. and Lunde, J., Engineering classification of jointed rock mass for the design of tunnel support. *Rock Mech*., 1974, **6**(4), 189–239.
14. Bieniawski, Z. T., Rock mass classification in rock engineering. In *Exploration for Rock Engineering*. In Proc. of the Symp. (ed. Bieniawski, Z. T.), Balkema, Cape Town, South Africa, 1976, vol. 1, pp. 97–106.
15. Sheorey, P. R., Application of modern rock classification in coal mines roadways. In *Comprehensive Rock Engineering*, Pergamon Press, Oxford, UK, 1993, pp. 411–431.
16. Zivor, R., Vilhelm, J., Rudajev, V. and Lokajíček, T., Measurement of *P*- and *S*-wave velocities in a rock massif and its use in estimating elastic moduli. *Acta Geodyn. Geomater.*, 2011, 8, **2**(162), 157–167.
17. Verma, D., Kainthola, A., Singh, R. and Singh, T. N., An assessment of geo-mechanical properties of some Gondwana coal using *P*-wave velocity. *Int. Res. J. Geol. Min.*, 2012, **2**(9), 261–274.
18. Venkateswarlu, V., Ghosh, A. K. and Raju, N. M., Rock mass classification for design of roof support – a statistical evaluation of parameters. *Min. Sci. Technol.*, 1989, **8**, 97–108.
19. Sheorey, P. R., A theory of *in situ* stresses in isotropic and transversely isotropic rock. *Int. J. Rock Mech. Min. Sci*., 1994, **31**, 23–34.

ACKNOWLEDGEMENTS. We thank the management of different mines for providing an opportunity to conduct this study. We also thank the Director, Indian Institute of Technology (Indian School of Mines), Dhanbad and the Director, Central Institute of Mining and Fuel Research, Dhanbad for providing the necessary facilities and support. This work is a part of the Ph D of A.P. being carried out at IIT (ISM), Dhanbad, Jharkhand.

Received 17 May 2017; revised accepted 16 February 2018

doi: 10.18520/cs/v114/i10/2167-2174